Contrib Mineral Petrol (1992) 111:194–202

Contributions to Mineralogy and Petrology
© Springer-Verlag 1992

Evidence for the trapped liquid shift effect in the Mount Ayliff Intrusion, South Africa

R. Grant Cawthorn, Bernhard K. Sander and Ian M. Jones

Department of Geology, University of the Witwatersrand, Private Bag 3, Wits 2050, South Africa

Received July 15, 1991/Accepted January 4, 1992

Abstract. Postcumulus trapped liquid shift in layered complexes produces cumulate minerals with more fractionated compositions than the original primary phases. This effect is shown by olivine compositions from the base of the Mount Ayliff Intrusion, where varying proportions of olivine to interstitial liquid produce a suite of rocks which define a tight linear trend on a binary whole-rock plot of MgO versus FeO. Extrapolation of this trend constrains the composition of the primary cumulus olivine to the range Fo_{84-86}, whereas olivine actually present have compositions Fo_{77-83}. The magnitude of the discrepancy between the theoretical and observed olivine compositions correlates directly with the weight fraction of interstitial liquid. These observations are quantitatively predicted by the trapped liquid shift model. They also argue against significant migration of residual liquid. Trapped liquid shift is documented over a vertical interval of 60 m. It occurred in rocks lying only 1 m above the basal contact of the intrusion and hence must be a comparatively rapid process.

Introduction

Postcumulus processes undoubtedly affect the final whole-rock and mineral compositions of rocks in layered complexes. However, the extent of such reactions is difficult to quantify because original cumulus mineral compositions and primary porosity cannot usually be independently determined. Furthermore, various scenarios have been postulated for the reaction between cumulus minerals and intercumulus liquid. It has also been debated whether the intercumulus liquid is trapped or migrates relative to the cumulus minerals (Irvine 1978, 1980, Tait et al. 1984). These models may be complementary, with different processes operative in different intrusions or at different stratigraphic levels in the same intrusion.

Barnes (1986) made quantitative calculations of the effect on cumulus mineral compositions reacting with varying proportions of intercumulus liquid. His model assumed that the liquid remained trapped relative to the cumulus crystals; and termed the change in mineral composition the "trapped liquid shift". Barnes (1986) presented several examples where the patterns of mineral compositions in short vertical sections in layered complexes did not fit with simple fractional crystallization of a single liquid, but were consistent with superimposed trapped liquid shift. He specifically referred to the Insizwa lobe of the Mount Ayliff Intrusion and suggested that the reverse upward differentiation in olivine compositions near the base of the intrusion could be explained by reaction with progressively decreasing proportions of trapped liquid.

Paktunc (1987) and Chalokwu and Grant (1987) have also argued that changes in primary olivine compositions have occurred, based on correlation between mode and whole rock composition. Similarly, Mathison and Booth (1990) have documented changes in pyroxene compositions.

Here, we present whole-rock data from several profiles through the Mount Ayliff Intrusion which permit an independent determination of the primary olivine composition. This can then be compared with the actual compositions of minerals present in the rock.

Theory

The magnitude of the trapped liquid shift correlates with the proportions of cumulus phases and trapped liquid (Barnes 1986). We use an oxide variation diagram to illustrate this process and then present data to test the extent of this effect. Olivine accumulation is the simplest situation to represent geometrically (Fig. 1), as the olivine compositions can be related to that of the liquid by the equations of Roeder and Emslie (1970). Liquid L^C crystallizes olivine F^C and produces a package of liquid plus crystals, of bulk composition B. Reaction with residual liquid continuously changes the olivine composition to lower Fo contents down to the solidus. The effect is that the tie-line joining instantaneous liquid and crystal composition rotates (from L^CF^C, through L^SF^S to L^RF^R). If the interstitial liquid remains trapped, rotation pivots about the bulk composition (if the trapped liquid can migrate

this constraint no longer applies and rigorous calculations become impossible). For a package containing a large proportion of olivine (B^1), the effect on the final olivine composition will be small (tie-line L^1F^1). Conversely, if the package has a small proportion of olivine (B^2), the effect will be greater (L^2F^2).

In most layered complexes the weight per cent of trapped liquid does not vary greatly over small vertical intervals, and so a wide range of bulk compositions is rarely available for study. In the theoretical example of Fig. 1 there is a large variation in the olivine to liquid proportions and so it is possible to determine the primary, cumulus composition of the olivine (F^C) by extrapolation through all the bulk compositions (B^1, B and B^2). Hence, the original primary composition (determined by construction) can be compared with the observed composition (determined by mineral analysis). In this way, an independent test of the extent of the trapped liquid shift is available. There are two restrictions and complications which limit the general applicability of this model. If there is more than one cumulus silicate phase, then the bulk composition is constrained within a triangle, not along a straight line, and precise prediction of primary compositions is not possible. Second, if a long vertical section of cumulates is considered, the primary composition of the cumulus phase may change due to differentiation. The bulk compositions would then no longer define a linear trend, as is shown in Fig. 2, where a series of packages is produced from a differentiating liquid ($L^1 - L^3$), such that the olivines range from $F^1 - F^3$. In Fig. 2 the bulk rocks (B^1, B^2, B^3) have a constant weight proportion of olivine to liquid of 2, but if they have random proportions they would scatter along their respective tie-lines and give an apparently meaningless distribution of points. If a short vertical interval within the intrusion is investigated, as is the case here, this effect may be minimal.

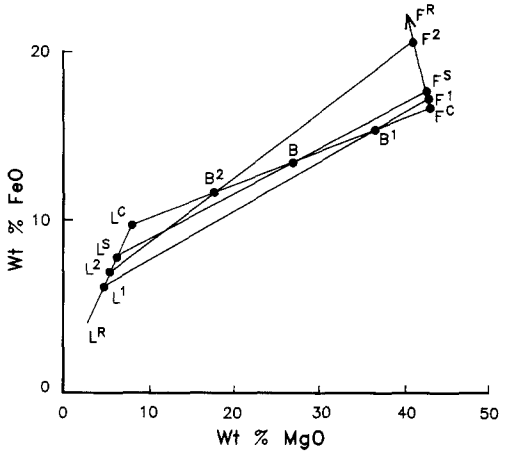

Fig. 1. MgO versus FeO variation diagram (wt%) illustrating the geometrical relations between liquid (L) and olivine (F), using the equations of Roeder and Emslie (1970), and range of possible bulk rock (B) compositions

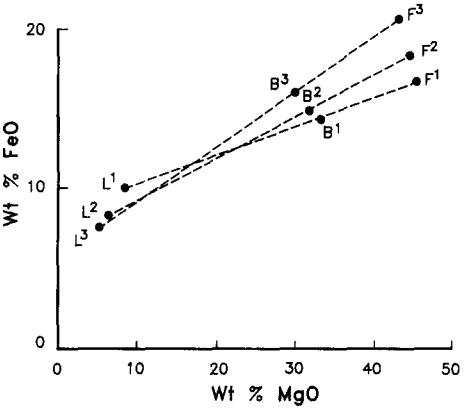

Fig. 2. MgO versus FeO variation diagram (wt%) illustrating the range of cumulates formed during differentiation. Liquid L^1 crystallizes olivine F^1 producing a bulk rock B^1. As the liquid differentiates it changes to L^2, the olivine to F^2, and the bulk rock to B^2. Each cumulate rock is arbitrarily shown containing 66 wt% olivine

Mount Ayliff Intrusion

The geology of this 1 km thick intrusion (Fig. 3) has been described in numerous papers (Scholtz 1963; Lightfoot and Naldrett 1984; Lightfoot et al. 1984, 1987; Cawthorn et al. 1985, 1986, 1988, 1991), and is not repeated here. At the base of the intrusion there is a discontinuous picrite horizon, up to 300 m thick, which contains cumulus olivine and chromite in the ratio 98.5 to 1.5. There is generally an underlying olivine gabbronorite, reaching 15 m thick at Waterfall Gorge (Lightfoot et al. 1984), but at Mount Evelyn it is less than 3 m. It has variable proportions of cumulus olivine (Fig. 4) and chromite, with abundant subhedral plagioclase and anhedral pyroxenes.

Geochemistry

We have taken eleven profiles through the picritic facies of the Tonti and Insizwa lobes of the intrusion (Fig. 3). Exposure permitting, whole-rock analyses have been obtained at typically 20 m intervals in the picrite, and at closer intervals in the underlying olivine gabbronorite. Representative data are presented in Table 1 and Figs. 4 and 5. In some instances olivine has been analysed by electron microprobe (Lightfoot et al. 1984, Cawthorn et al. 1986), but in most cases the olivine has been separated and analysed by XRF spectrometry. Multiple electron microprobe analyses and traverses across single grains of olivine have shown that the olivine is homogeneous (Cawthorn et al. 1986), and so direct comparison with the XRF data is possible. For the Mount Evelyn section electron microprobe analyses give consistently higher totals and higher Fo values than XRF analyses (Table 1). The latter is due to the inclusions of chromite and sulphide in olivine which cannot be mechanically separated. Plots of olivine compositions versus height have been presented by Cawthorn et al. (1986). Typically Fo increases upwards through the bottom 10–30 m, as does the modal olivine content (Fig. 4). Thereafter it either remains constant or decreases. Data from the basal section with the largest range in whole-rock MgO contents from the old mine adits at Waterfall Gorge (Lightfoot and Naldrett 1984; Lightfoot et al. 1984; this study) are shown in Fig. 4A. Olivine changes from Fo_{77} to Fo_{81} upwards over 20 m. All incompatible trace elements, as exemplified by Zr in Fig. 4, show a decrease upwards, reflecting a decreasing proportion of trapped liquid. Lightfoot and Naldrett (1984) give comparable plots for other incompatible trace and major elements. There is a slight reversal in both olivine and trace element trend at 5–8 m. A comparable, though less detailed, section through the Mount Evelyn profile is also presented in Fig. 4B. This too shows a break in olivine

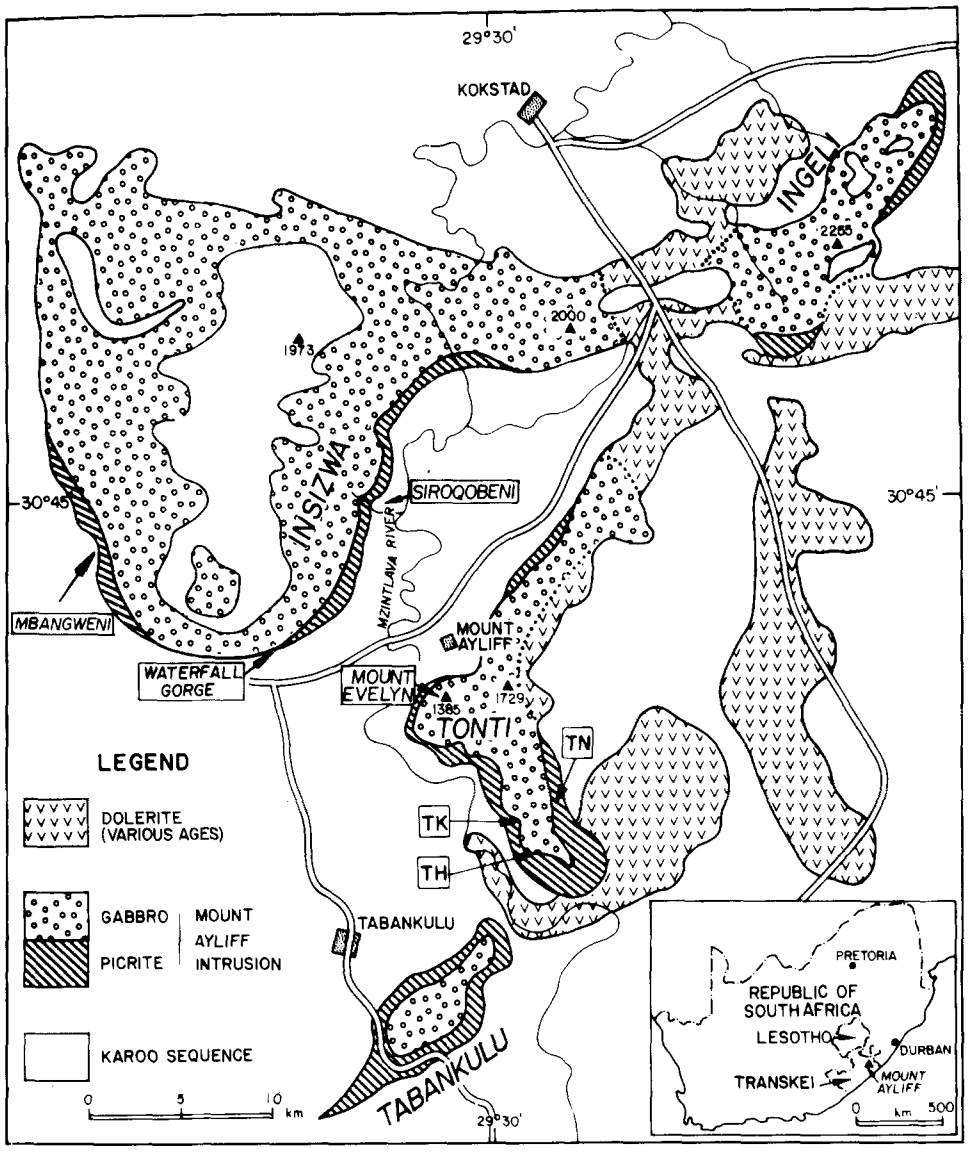

Fig. 3. Simplified geological map of the Mount Ayliff Intrusion showing the locations of the profiles sampled through the picrite documented in this study at Waterfall Gorge, Mbangweni and Siroqobeni in the Insizwa lobe; and Mount Evelyn, TN, TH and TK in the Tonti lobe

and Zr trends, but at a greater height than in the Waterfall Gorge section.

Models for producing reversals in mineral compositions

Basal reversals in mineral compositions are not unusual in layered complexes and several mechanisms have been invoked to explain specific examples. These hypotheses are discussed here in relation to the Mount Ayliff Intrusion.

(1) Addition of less differentiated magma

Addition of less differentiated magma will cause a reversal in mineral compositions. The reversal could be gradational if there is mixing with resident magma, or upward migration of underlying, low density interstitial liquid, as observed in the Muskox Intrusion (Irvine 1980). However, in the case of the reversal in Fig. 4, there are no underlying cumulates from an earlier magma, and so this model cannot apply.

(2) Addition into a zoned magma

Wilson et al. (1987) documented gradual reversals in mineral composition which are transgressive to the modal layering. Their model requires gradual intrusion of less differentiated magma into a zoned magma chamber, which was crystallizing on an inclined floor. In the case of the Mount Ayliff Intrusion, while there are variations in the topographic elevation of the basal contact, the olivine compositions do not change systematically with these variations in height as in the Fongen-Hyllingen Intrusion. These observations argue against the existence of a zoned magma chamber.

Table 1. Chemical analyses of whole-rock and olivine compositions from profiles through the olivine cumulate sequence of the Mount Ayliff Intrusion.

	Mount Evelyn Profile–Tonti lobe							
Sample	Pr21/1	Pr21/2	Pr21/3	Pr21/4	Pr21/5	Pr21/6	Pr21/7	Pr21/8
Height(m)	1	3	6	10	14	19	35	52
Whole rock (weight percent)								
SiO_2	47.5	44.4	43.6	42.1	42.8	42.2	41.9	43.8
TiO_2	.71	.41	.30	.20	.25	.24	.15	.28
Al_2O_3	10.1	5.9	5.7	5.0	4.9	4.9	5.0	4.7
Fe_2O_3	11.8	14.3	14.5	14.4	14.5	14.6	15.1	16.0
MnO	.2	.2	.2	.2	.2	.2	.2	.2
MgO	19.5	29.9	31.7	33.3	34.4	33.2	34.2	32.8
CaO	6.8	3.7	3.4	3.1	3.0	3.0	2.9	3.4
Na_2O	1.78	1	.91	.81	.77	.77	.63	.74
K_2O	.49	.37	.25	.13	.16	.15	.07	.13
P_2O_5	.11	.07	.06	.05	.07	.05	.04	.06
Total	99.0	100.2	100.6	99.3	101.2	99.3	100.2	102.2
Trace elements (ppm)								
Ba	162	144	78	50	57	59	36	51
Rb	13	10	5	2	7	2	4	6
Sr	198	70	63	52	63	60	63	57
Y	24	14	9	7	8	8	6	8
Zr	72	35	20	11	39	35	27	34
Nb	6	0	0	1	2	1	0	2
Cu	113	121	130	155	81	157	114	103
Co	55	117	120	127	128	131	139	129
Ni	344	710	663	671	848	1298	514	405
Zn	87	98	96	92	94	92	91	105
V	228	198	170	171	129	161	116	123
Cr	1558	4128	4273	4027	5136	6542	4166	2873
S	920	1040	560	1710	700	1570	1580	1390
Olivine compositions (weight percent)								
Technique	XRF	Probe	XRF	Probe	Probe	Probe	XRF	XRF
SiO_2	39.9	38.8	37.5	39.1	39.3	39.2	38.5	37.9
TiO_2	.65	–	.77	–	–	–	.28	.42
Al_2O_3	1.6	.01	1.0	.02	.02	.02	1.1	.4
FeO*	18.1	17.6	17.3	16.1	15.9	15.7	16.3	18.7
MnO	.2	.2	.2	.2	.2	.2	.2	.2
MgO	36.9	43.3	40.2	44.5	44.7	44.8	41.2	40.6
CaO	1.0	.11	.4	.09	.10	.08	.5	.2
Total	98.3	100.3	97.3	100.1	100.4	100.1	98.1	98.5
Fo mol%	78.5	81.4	80.5	83.1	83.4	83.5	81.8	79.5
Trace elements (ppm)								
Ni	900	930	860	610	1100	1300	610	= 510
Mode % Olivine	37	68	64	78	74		78	65

(3) Supercooling and/or rapid cooling

Dynamic crystallization experiments, especially on lunar basalts (reviewed by Lofgren 1980), have produced strongly zoned olivine crystals, whose bulk composition becomes depleted in Fo as cooling rate increases. By analogy, rapidly cooled margins of intrusions could contain anomalously Fo-depleted olivine. However, at cooling rates sufficient for this effect to become significant olivine crystals would no longer be euhedral (Donaldson 1976). Furthermore, cumulate rocks, with up to 60% olivine, could not be produced in a magma chamber which is cooling at those rates.

While all the above mechanisms can and probably do occur in specific instances, they do not fit the observations on reverse differentiation of the olivine compositions at the base of the Mount Ayliff Intrusion.

Trapped liquid shift model

Typical whole-rock data from Mount Ayliff are plotted in Fig. 5. Before interpreting these in detail, it is necessary to discuss some minor recalculations of the data. The FeO content, plotted in Fig. 5, is calculated from XRF analyses by assuming that the Fe_2O_3 to FeO ratio varies from zero in a pure olivine cumulate to 0.1 in magma. Chromite and sulphide accumulation will increase the whole-rock FeO content, relative to an olivine-liquid mixing line. It is therefore assumed that all the Cr in the analysis is in

Table 1. (continued)

	Mbangweni profile–Insizwa lobe						
Sample	Pr12/1	Pr12/2	Pr12/3	Pr12/5	Pr12/6	Pr12/7	Pr12/8
Height (m)	.50	7	15	32	43	55	86
Whole rock (weight percent)							
SiO_2	52.0	48.9	44.8	44.6	44.5	44.3	44.3
TiO_2	.77	.56	.37	.43	.32	.22	.27
Al_2O_3	12.6	9.8	5.3	6.8	4.2	4.9	3.9
Fe_2O_3	11.4	11.9	14.6	14.2	14.9	13.9	14.9
MnO	.2	.2	.2	.2	.2	.2	.2
MgO	10.4	19.7	28.4	28.3	30.5	31.8	32.2
CaO	9.7	7.1	4.3	4.3	4.1	4.5	3.9
Na_2O	1.84	1.87	1.07	1.22	.84	.74	.71
K_2O	.63	.53	.17	.26	.13	.09	.10
P_2O_5	.10	.10	.04	.08	.05	.04	.04
Total	99.7	100.4	99.2	100.2	99.8	100.6	100.6
Trace elements (ppm)							
Ba	171	145	78	99	59	36	40
Rb	17	15	6	11	4	5	4
Sr	99	76	76	92	51	60	49
Y	22	15	12	13	10	10	9
Zr	69	55	42	54	36	29	31
Nb	1	2	3	2	3	1	1
Cu	69	76	182	269	123	149	83
Co	41	72	111	121	124	124	128
Ni	153	455	831	946	894	1019	1084
Zn	89	84	91	95	110	83	96
V	254	187	138	134	141	99	115
Cr	566	1142	2482	2695	2566	2568	2225
S	550	550	1150	1580	870	940	1040
Olivine compositions (weight percent)							
SiO_2		38.6	38.3	37.9	38.2	38.2	38.2
TiO_2		.36	.17	.37	.15	.09	.10
Al_2O_3		.7	.4	.8	.2	.3	.2
FeO*		20.5	18.9	18.5	18.4	16.2	17.4
MnO		.3	.2	.2	.2	.2	.2
MgO		38.1	42.1	41.2	42.7	44.2	42.4
CaO		.6	.3	.4	.2	.3	.2
Total		99.2	100.4	99.3	100.1	99.5	98.8
Fo mol%		76.8	79.9	79.9	80.5	83	81.3
Trace elements (ppm)							
Ni		1200	1320	1450	1370	1470	1570

chromite, and an appropriate weight of chromite is subtracted from the analysis using the chromite analyses of Cawthorn et al. (1991). Similarly all Cu is assumed to be in sulphide, the composition of which has been estimated by Lightfoot et al. (1984); and an appropriate weight of FeO removed from the whole-rock analysis. The analysis is then recalculated to its original total. Comparison in Fig. 5 of the original analysis with the composition recalculated after removal of the chromite and sulphide component demonstrates that these corrections make little difference to the data, and have little effect on the subsequent discussion.

(1) Primary olivine compositions

The most convincing linear trend of whole rock analyses is obtained for the Waterfall Gorge section as it displays the greatest range of MgO contents. A common line is plotted on all the diagrams to show that the data for all profiles are broadly similar. One sample analysed by Eales (1980) from a borehole drilled 20 km north-east of Waterfall Gorge is included and is distinctly lower in FeO. This may suggest that there is a different parental magma involved in the formation of this section.

It is apparent that the compositions of the olivine obtained both by electron microprobe and XRF are distinctly enriched in iron compared to that predicted by the linear relationship displayed by the whole rock data. In Fig. 5, the data for Waterfall Gorge of Lightfoot and Naldrett (1984) are slightly enriched in FeO compared to the present data, which is partly due to the fact that Cr is not quoted and so no correction for chromite can be applied. From the trends in Fig. 5 it is estimated that the cumulus olivine composition ranges from Fo_{84} using the

Table 1. (continued).

	Siroqbeni profile–Insizwa lobe								
Sample	Pr16/0	Pr16/1	Pr16/2	Pr16/3	Pr16/4	Pr16/5	Pr16/6	Pr16/7	Pr16/8
Height(m)	2	7	21	27	40	60	87	101	124
Whole rock (weight percent)									
SiO_2	48.2	45.6	43.5	43.4	43.2	42.7	43.3	41.9	43.2
TiO_2	.65	.42	.27	.30	.30	.26	.35	.23	.27
Al_2O_3	10.1	7.8	5.1	5.3	4.9	5.0	5.2	5.2	5.1
Fe_2O_3	11.9	12.9	13.9	14.1	14.5	14.5	15.1	15.0	14.0
MnO	.2	.2	.2	.2	.2	.2	.2	.2	.2
MgO	20.0	25.9	32.9	31.6	32.4	33.8	31.4	32.5	33.7
CaO	6.5	5.1	3.3	3.5	3.3	3.3	3.5	3.5	3.4
Na_2O	1.75	1.39	.95	.92	.90	.86	2.21	.90	1
K_2O	.52	.29	.17	.17	.21	.16	.23	.09	.09
P_2O_5	.11	.07	.05	.05	.06	.05	.06	.04	.04
Total	99.9	99.8	100.3	99.5	100	100.8	101.5	99.7	101.0
Trace elements (ppm)									
Ba	154	95	62	61	68	60	70	46	78
Rb	19	11	11	7	11	9	5	6	8
Sr	126	93	61	63	64	63	61	62	68
Y	20	12	9	8	9	10	6	7	11
Zr	76	53	41	35	41	38	30	31	41
Nb	6	2	3	2	4	3	2	2	4
Cu	82	76	249	238	242	422	180	370	375
Co	72	94	128	115	125	134	127	140	137
Ni	593	862	1187	1078	1067	1494	1376	1325	1112
Zn	86	84	86	81	89	80	83	87	86
V	183	142	117	111	111	104	124	102	134
Cr	1806	2588	3254	3185	2970	2947	4825	3954	3844
S	730	650	1550	1550	1150	2170	850	1970	2700
Olivine compositions (weight percent)									
SiO_2	42.8	41.1	39.0	38.9	38.7	39.9	38.6	38.6	38.6
TiO_2	.56	.32	.37	.31	.28	.27	.17	.33	.27
Al_2O_3	1.8	1.8	.7	1.0	.9	.7	.5	.8	.3
FeO*	17.6	16.4	16.0	16.1	16.7	15.9	16.0	17.7	17.2
MnO	.2	.2	.2	.2	.2	.2	.3	.2	.3
MgO	34.8	38.1	41.8	40.2	41.8	42.1	43.0	40.8	41.9
CaO	2.2	1.5	.3	.6	.2	.4	.2	.3	.2
Total	100	99.5	98.5	97.4	98.8	99.4	98.7	98.7	98.7
Fo mol%	77.9	80.6	82.3	81.6	81.7	82.5	82.7	80.5	81.3
Trace elements (ppm)									
Ni	1210	1370	1520	1590	1450	1910	1750	1670	1200
Mode % Olivine	46	63	61		70	69	65	66	62

Analyses of olivine by XRF on mineral separates except where indicated as electron microprobe analysis.

uncorrected data of Lightfoot Naldrett (1984) to greater than Fo_{86} from the analyses of Eales (1980).

(2) Magnitude of trapped liquid shift

The actual analysed olivine compositions range from Fo_{77-83}, and so cannot represent the primary compositions. There can be little doubt that the trapped liquid shift has rotated the tie-lines between olivine and residual liquid during postcumulus crystallization to produce the observed spread of olivine compositions (Fig. 5).

The magnitude of this trapped liquid shift can be assessed by examining the proportion of olivine in relation to its composition. The normative proportion of olivine, using the Fe_2O_3 to FeO ratios discussed previously, in the whole rock is plotted against analysed Fo content (Fig. 6), and shows an extremely good correlation, consistent with the predictions of Barnes (1986). Extrapolating to 100% olivine should define the composition of the primary olivine. This lies in the range Fo_{85-87}, and so is comparable to or slightly higher than predicted by Fig. 5. Eales (1980) also concluded, on the basis of chemical variation, that the primary composition of olivine in this intrusion was Fo_{86}.

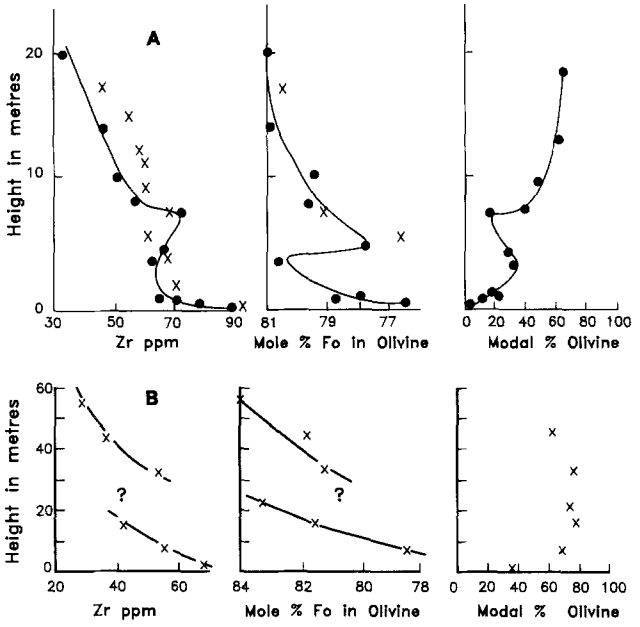

Fig. 4. Plot of whole-rock Zr content, modal percent olivine and olivine composition versus height above the base of the intrusion at Waterfall Gorge (Fig. 4A) and Mount Evelyn (Fig. 4B). The *circles* are from the data of Lightfoot and Naldrett (1984) and Lightfoot et al. (1984) and the *crosses* from our data. The contact of the lower olivine gabbronorite with picrite is gradational, but is taken where olivine exceeds 60 modal percent

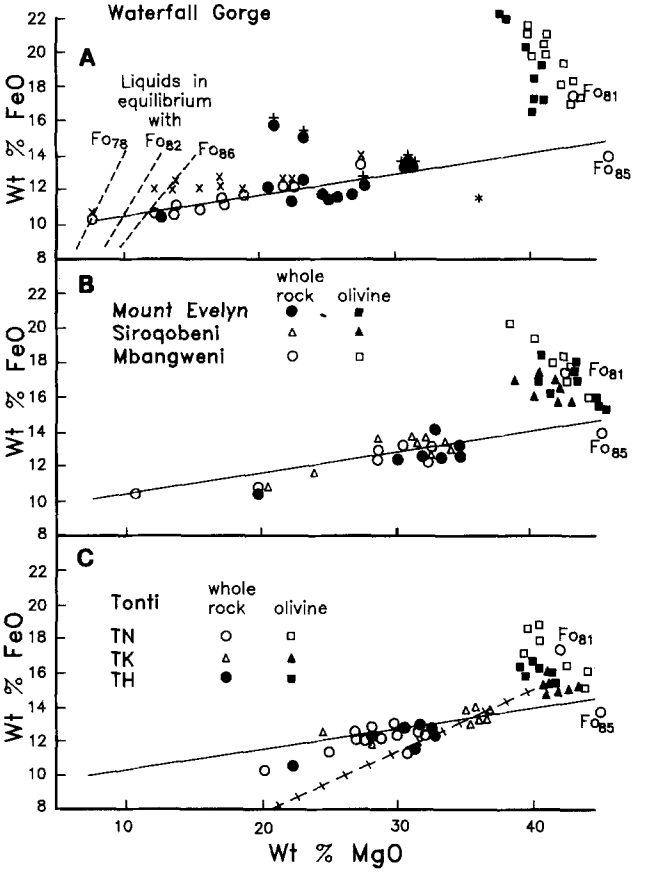

Fig. 5 A, B, C. MgO versus FeO variation diagrams (wt%) for whole-rock and olivine compositions for profiles through the Mount Ayliff Intrusion. Compositions Fo_{85} and Fo_{81} are shown as *circles* for reference. Compare this diagram with Fig. 1. **Fig. 5A** shows the data for the Waterfall Gorge section. *Crosses* are the original data from Lightfoot and Naldrett (1984), while the *open circles* show the same analyses corrected for Fe in sulphide. *Solid circles* show the analyses (this study) recalculated with Fe in chromite also removed. A few original analyses are shown as *pluses* to illustrate the magnitude of this recalculation. *Asterisk* is from Eales (1980). *Open squares* are olivine analyses from Lightfoot et al. (1984) by electron microprobe, and *solid squares* are from this study by XRF analysis on mineral separates. *Dashed lines* show the ranges of compositions of liquids in equilibrium with olivine of different composition as defined by the equations of Roeder and Emslie (1970). **Fig. 5B** contains data from Mbangweni (*open symbols*), Mount Evelyn (*closed symbols*), and Siroqobeni (*triangles*). Total FeO in chromite has been subtracted from the whole-rock data. **Fig. 5c** contains data from profile TN (*open square* and *circle*), TH (*closed square* and *circle*) and TK (*triangles*). An identical *solid line* is given in each diagram for reference. The *hachured line* shows the trend would be inferred if a single suite of whole rock and olivine compositions (from profile TK) showing little variation in the proportion of trapped liquid were investigated. The inferred parental liquid extrapolated from observed olivine compositons would project to impossibly low FeO contents.

(3) Trapped versus migrating interstitial liquid

The calculations of Barnes (1986) depend upon the interstitial liquid being trapped. If the interstitial liquid is free to migrate then the extent of reaction cannot be predicted. For example, had there been channelways within the crystal mush along which relatively large volumes of liquid migrated, a major effect on the cumulus mineral compositions would be predicted, even though the final apparent porosity of that rock need not be particularly high. Eales (1980) recorded one isolated sample of picrite anomalously enriched in certain incompatible elements which he attributed to local enrichment in interstitial liquid, indicating that such processes may occasionally occur and are recognisable from trace element analysis. If movement of interstitial liquid had happened on a significant scale there would be a very poor correlation in Figs. 4 and 6. The fact that data on those figures are tightly constrained suggests that liquid migration has been minimal.

(4) Differentiation

The effects of differentiation and trapped liquid shift can be compared in a plot of Fo versus Ni content of olivine (Fig.7). Barnes (1986) calculated how these should be related during magmatic fractionation. The compositions of primary olivine are shown by the trend marked "adcumulate" in Fig. 7, indicating that if they formed a true adcumulate rock these would be the preserved compositions. Formation of a mesocumulate rock would permit changes in the olivine composition by trapped liquid shift to those marked "30% trapped liquid". The change for a specific olivine composition is shown by the line from P (primary mineral) to R (reequilibrated mineral). The data for the Mount Evelyn profile are included in Fig. 7 and parallel the trend PR. This suggests that the variation in

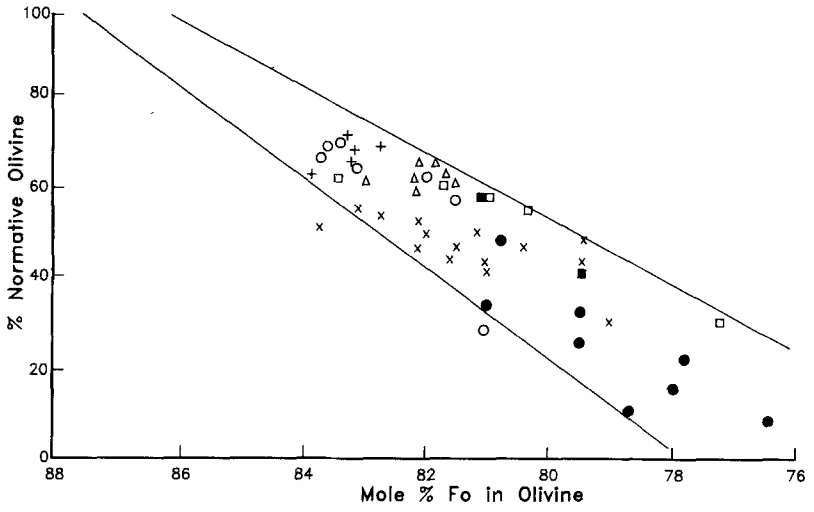

Fig. 6. Plot of Fo content in olivine versus normative proportion of olivine in bulk rock. This shows that the greater the proportion of olivine in the rock the smaller the change in olivine composition from its presumed primary composition of Fo_{84-86}, as predicted by Fig. 5. Where olivine is least abundant samples show a shift in composition of up to 9 mol% Fo. All the samples define a fairly restricted trend. Had there been migration rather than trapping of residual liquid greater scatter of the data would be expected. Symbols: *solid circles*, Waterfall Gorge; *open circles*, Mount Evelyn; *open squares*, TH; *triangles*, TN; *pluses*, TK; *crosses*, Mbangweni; *solid squares*, Siroqobeni

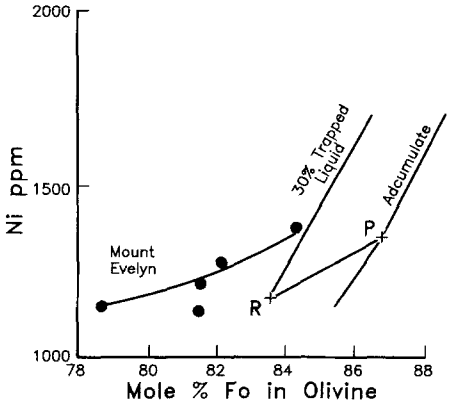

Fig. 7. Plot of Ni (ppm) in olivine versus Fo content of olivine, for Mount Evelyn profile (*solid circles*). "Adcumulate" and "30% trapped liquid" trends are taken from Barnes (1986), and refer to calculated compositions of primary olivine and the resultant change due to trapped liquid shift assuming 30% by weight of interstitial liquid. Points *P* and *R* refer to a specific primary and reequilibrated olivine composition demonstrating direction and magnitude of trapped liquid shift

compositions could be explained by changes in the proportion of trapped liquid, but starting with a slightly different parental composition from that used by Barnes. Differentiation would produce a trend parallel to the "adcumulate" or "30% trapped liquid" curves, which is not observed in the data. Hence, it would appear that the extent of differentiation is not significant in relation to the effect of trapped liquid shift.

(5) Parental magmas

The range of liquid compositions in equilibrium with the calculated primary olivine compositions (Fo_{84-86}) can be determined from the equations of Roeder and Emslie (1970), and is plotted in Fig. 5. The intersection of these liquid trends with the bulk-rock trend constrains the composition of the parental magma. If the primary olivine is Fo_{86}, the parental magma must contain 10.8% MgO at 10.5% FeO.

It is important to note that if a trend is extrapolated from the cluster of analysed olivine compositions through the cluster of whole rock compositions for profile TK (for example), an apparent parent magma would be inferred which is extremely depleted in FeO (4.5% FeO at 5% MgO). From the above discussion it can be inferred that this represents the composition of the residual liquid as it reequilibrated with the olivine, not the parental magma.

Conclusions

An independent test for the trapped liquid shift of Barnes (1986) is presented. This test is possible because a suite of rocks has been sampled which displays a wide range of cumulus to liquid proportions within a short vertical interval. It is aided by the fact that there is only one major cumulus silicate phase - olivine. Whole-rock analyses from the picritic zone of the Mount Ayliff Intrusion define a linear MgO-FeO trend, which can be extrapolated to constrain the composition of the primary cumulus olivine (Fo_{84-86}). This primary composition differs markedly from the compositions actually observed in the same rocks (Fo_{77-83}), verifying the trapped liquid shift hypothesis. The extent of the shift in composition is directly related to the ratio of interstitial liquid to olivine; a consequence of the trapped liquid shift model, as distinct from models which permit residual liquid to migrate vertically. The largest shift occurs for a sample taken only 1 m above the basal contact of the intrusion where cooling would have been rapid. Hence, this reaction with trapped liquid is a rapid phenomenon.

The apparent reverse differentation trend, which is attributed to trapped liquid shift, can be traced upwards for 60 m in the Mount Evelyn profile. This is very much less than the 400 m of the Stillwater Complex over which Raedeke and McCallum (1984) reported a similar reverse trend, and for which a similar process was invoked.

As a result of the rotation of tie-lines in oxide binary diagrams due to the trapped liquid shift, an incautious or

poorly constrained interpretation of a suite of cumulates and their observed cumulus composition could yield an erroneous inferred parental liquid composition.

Acknowledgements. Logistical support in southern Tonti to IMJ was generously provided by Johannesburg Consolidated Investments Co. Ltd. Financial support to RGC and BKS from the Foundation for Research and Development (South Africa) is gratefully acknowledged. Drs SJ Barnes, CI Mathison and FJ Kruger reviewed an earlier draft of this manuscript. Geochemical, drafting, photographic and secretarial assistance was provided by Ms N Day, Ms L Whitfield, Mr M Hudson and Ms J Wilmot.

References

Barnes SJ (1986) The effect of trapped liquid crystallization on cumulus mineral compositions in layered intrusions. Contrib Mineral petrol 93:524–531

Cawthorn RG, Groves DI, Marchant T (1985) Magnesian ilmenite: clue to high-Mg parental magma of the Insizwa intrusion, Transkei. Can Mineral 23:609–618

Cawthorn RG, de Wet M, Maske S, Groves DI, Cassidy KF (1986) Nickel sulphide potential of the Mount Ayliff Intrusion (Insizwa Complex) Transkei. S Afr J Sci 82:572–576

Cawthorn RG, Maske S, de Wet M, Groves DI, Cassidy KF (1988) Contrasting magma types in the Mount Ayliff Intrusion (Insizwa Complex), Transkei: evidence from ilmenite compositions. Can Mineral 26:145–160

Cawthorn RG, de Wet M, Hatton CJ, Cassidy KF (1991) Titanium-rich chromite from the Mount Ayliff Intrusion: further evidence for high titanium tholeiitic magma. Am Mineral 76:561–573

Chalokwu CI, Grant NK (1987) Reequilibration of olivine with trapped liquid in the Duluth Complex, Minnesota. Geology 15:71–74

Donaldson CH (1976) An experimental investigation of olivine morphology. Contrib Mineral Petrol 57:187–213

Eales HV (1980) Contrasted trace-element variations in two Karroo cumulus complexes. Chem Geol 29:39–48

Irvine TN (1978) Infiltration metasomatism, adcumulus growth, and secondary differentiation in the Muskox Intrusion. Carnegie Inst Washington Yearb 77:743–751

Irvine TN (1980) Magmatic infiltration metasomatism, double-diffusive fractional crystallization, and adcumulus growth in the Muskox Intrusion and other layered intrusions. In: Hargraves RB (ed) Physics of magmatic processes. Princeton University Press, New Jersey, pp 326–383

Lightfoot PC, Naldrett AJ (1984) Chemical variation in the Insizwa Complex, Transkei, and the nature of the parent magma. Can Mineral 22:111–123

Lightfoot PC, Naldrett AJ, Hawkesworth CJ (1984) The geology and geochemistry of the Waterfall Gorge section of the Insizwa Complex with particular reference to the origin of the nickel sulfide deposits. Econ Geol 79:1857–1879

Lightfoot PC, Naldrett AJ, Hawkesworth CJ (1987) Re-evaluation of chemical variation in the Insizwa Complex, Transkei. Can Mineral 25:79–90

Lofgren GE (1980) Experimental studies on the dynamic crystallization of silicate melts. In: Hargraves RB (ed) Physics of magmatic processes. Princeton University Press, New Jersey, pp 487–551

Mathison CI, Booth RA (1990) Macrorhythmically layered gabbronorites in the Windamurra gabbroid body, Western Australia. Lithos 24:171–180

Paktunc AD (1987) Differentiation of the Cuthbert Lake ultramafic dikes and related mafic dikes. Contrib Mineral Petrol 97:405–416

Raedeke LD, McCallum IS (1984) Investigations in the Stillwater Complex: Part II. Petrology and petrogenesis of the Ultramafic series. J Petrol 25:395–420

Roeder PL, Emslie RF (1970) Olivine–liquid equilibrium. Contrib Mineral Petrol 29:257–289

Scholtz DL (1936) The nickeliferous ore deposits of East Griqualand and Pondoland. Trans Geol Soc S Afr 39:81–210

Tait SR, Huppert HE, Sparks RSJ (1984) The role of compositional convection in the formation of adcumulate rocks. Lithos 17:139–146

Wilson JR, Menuge JF, Pedersen S, Engell-Sorensen O (1987) The Southern part of the Fongen–Hyllingen layered mafic complex, Norway: emplacement and crystallization of compositionally zoned magma. In: Parsons I (ed) Origins of igneous layering. Reidel, Dordrecht, pp 145–184

Editorial responsibility: R. Binns